Ionospheric Propagation, Transmission Lines, & Antennas

for the

QRP DX'r

Adrian Weiss W0RSP

Milliwatt QRP Books

810 Placita La Canoa, Green Valley, AZ 85614

aweiss@usd.edu

Adrian Weiss W0RSP's new long-awaited book, **IONOSPHERIC PROPAGATION, TRANSMISSION LINES, and ANTENNAS for the QRP DX'r**, will be introduced at Dayton 2011 in the searchable-PDF format on CD. The author provides the following description:

The book examines the significant factors that influence the strength and coverage of a QRP h.f. signal on its journey from transmitter to distant receiver, with special attention to QRP DX'ing. Chapter 1 is an overview in which various types of loss factors are interrelated including the antenna systems at both ends and the nature of the ionospheric path itself. The tedious down-and-dirty details, data and theories (and a *few* formulae) are discussed in later chapters. Pages 26 to 52 of Chapter 1 are devoted to an explanation of the application of current MUF3000 contour maps available on the WEB and seven recommended propagation analysis software programs (included on the CD).

Chapter 2, "Antennas, Transmission Lines, and SWR," is aimed at explaining the basic principles underlying h.f. traveling wave behavior in the antenna system. This includes a detailed explanation of the importance and methods of minimizing line loss (either intrinsic or from deterioration), impedance transformation along a transmission line, the resulting complex impedances, and the nature of antenna resonance and its minor importance in radiation efficiency. The chapter is grounded entirely in M. Walter Maxwell W2DU's (Head of Astro-Electronics Division of RCA, retired) conjugate matching theorem and explanations of antennas and feedlines as seen in his series of papers in *QST* and the 3 editions of his book **Reflections** (1990, 2001, and 2010 – the "bible", buy one!). Maxwell has edited this chapter and suggested revisions and provided an illustration. It represents what I have learned about these subjects from studying his work. Naturally, SWR myths and flawed antenna designs are targets and I aim to equip the QRP'r with the concepts that lead to sorting out the fallacies from the realities in order to achieve an efficient antenna system.

Chapter 3 explains the "Formation and Structure of the Ionosphere" as background for understanding the propagation of h.f. signals. Based upon research published in scientific journals (*Proceedings of the IEEE etc.),* topics include the photon-ionization process, solar variables controlling the ionosphere, zenith angle, D- and E-layer absorption, and the effect of the geomagnetic field upon F-layer behavior. This is somewhat complex technical material but the QRP DX'r ought to be aware of it – it is what makes QRP DX propagation happen.

Chapter 4 analyzes "The Propagation of H.F. Radio Signals in Real Ionopsheres" by discussing the refraction process and mechanics of oblique propagation, followed by ray traces of ham band signals in five real ionospheres, and concluding with a review of the ground-breaking ray-tracing work by deVoogt and Muldrew in the 1950's and 60's.

[CD (69 mB). PDF 8.5" x 11" format. Book Length: 349 pages,. Chap. 1: 52 pages, 27 illustrations, 3 tables. Chap. 2: 97 pages, 39 illustrations, 15 tables. Chap. 3: 95 pages., 63 illustrations, 5 tables. Chap. 4: 84 pages, 58 illustratons, 2 tables.

Ionospheric Propagation Transmission Lines

and

Antennas

for the

QRP DX'r

Adrian Weiss W0RSP

(ex-K8EEG)

author of

Joy of QRP: Strategy for Success

History of QRP in the US, 1924-60

The Milliwatt: National Journal of QRPp

Milliwatt QRP Books

810 Placita la Canoa

Green Valley, AZ, 85614

aweiss@usd.edu

2011

PREFACE

In the "Preface" to **The Joy of QRP: Strategy for Success,** dated January 1985, the first step leading to the completion of **Ionospheric Propagation, Transmission Lines and Antennas for the QRP DX'r** was explained as follows:

"A word about how this book came into its present form. I began writing it about five years ago [i.e. 1979], but what I came up with at first was a typical "pap and pablum" thing that didn't really explain anything. So I tossed that version out and committed myself to the task of addressing the needs of newcomers and veterans alike. What resulted was the massive typescript of **The QRP'rs Guide to Transmission Lines, Antennas, Propagation and DX'ing: The History, Theory and Practice of QRP**, running to 1150 double-spaced typed pages with nearly 300 drawings, many of them consisting of multiple curves. Three chapters totaling about 450 of those pages provided "hard-core" propagation theory and application, most of which has never been seen in the amateur literature before [*NB: or since, for that matter*]. *CQ Publishing* had waited patiently for the book, but in the meantime, had initiated publication of a new magazine, and budget and staff were strained to the limit. Rather than wait until things loosened up, I decided to pull out about 375 pages directed at newcomers, and **The Joy of QRP: Strategy for Success** is the result. We'll try to get the rest into print in the next year or so. Several individuals deserve a word of gratitude for their assistance in this project: Sylvia Wheeler, writer, poet and teacher, for comments on the first chapter of **The QRP'rs Guide**; Walter Maxwell (W2DU), Astro-Electronics Division of RCA, for corrections and suggestions for the antenna chapter of **The QRP'rs Guide**; and Robert B. Rose (K6GKU), Head, Naval lonospheric Assessment Systems Branch, for reading the entire(!) 1150 page typescript, making corrections and suggestions for the propagation, DX'ing and "PIanning for QRP Operation" chapters, and permitting me to include one of his previous articles from **The Milliwatt**…"

The QRP'rs Guide to Transmission Lines, Antennas, Propagation and DX'ing section of the massive typescript never saw the light of day despite my intentions. **The History of QRP in the US, 1924-1960** became my next book project, after which my professional research program (the various aspects of the printing operations – typefaces, specific type-fonts, papers and watermarks, compositors and printing shops, textual corruptions, the publication trade etc., which produced the books by Shakespeare and his contemporaries in Elizabethan England) began absorbing all my time and energy. Also, several readers of the manuscript thought it to be a bit too technical for the average QRP operator. I thought that I needed to know more about propagation than I did when I wrote the book. The micro-computer age arrived along with propagation programs like **MINIMUF** with which Bob Rose K6GKU introduced QRP'rs and other radio amateurs to the world of propagation-path analysis based upon the current 10.7cm solar flux as opposed to the 12-month smoothed average sunspot number. The 286 and then 386 and 486 CPU's increased the speeds of calculation and the amount of data that could be processed in increasingly reasonable amounts of time. As will be explained, some of these 286 DOS programs are still valuable primary tools for practical path analysis. The WEB became an "instant" source of ionospheric data along-side WWV's broadcasts 18 minutes after the hour. By 1997 or so when I talked about propagation to the NORCAL annual "Pacificon" QRP convention, I had the advantage of years of computer assisted propagation analysis as well as my earlier propagation reseach in scientific journals for **The QRP'rs Guide**. Going back through that material in preparation for the NORCAL presentation, I thought "Wow! Most of this stuff still hasn't shown up in the amateur radio publications! What a waste!". I retired in 2008 and in early 2010 Chuck Adams (founder of the *QRP-L* WEB site which had the phenomenal impact of putting all of us QRP'rs in instant contact – but without facebook pictures) unwittingly motivated me to pull out **The QRP'rs Guide** material and "fix it" for publication. The current state of scanner evolution and OCR software eliminated the major obstacle to preparing about 650 double-spaced type-written pages for printing. Likewise, an early Windows graphics program facilitated the production of relatively "professional" graphs and diagrams. And, above all, the cost of a text printed on paper was reduced to the price of a CD plus flat rate USPS postage and a bit for the work that produced it. All that remained was the bloody tedious work, which *did not include cutting corners* and omitting useful material because it would add to the cost of a printed book. I had more material and diagrams that could have been put in – including some really interesting stuff like backscatter propagation, spread-F, and Alouette I topside Nv soundings etc. But this book is a good start for average QRP'rs who want to understand what is happening once that signal crosses the junction between the final amplifier pinet output filter and the input terminals of the transmission line. Chapter 1 provides an overview which omits most of the tedious down-and-dirty details and data in the rest of the book. Then the serious reading begins with Chapter 2. When you are running 1 to 5 watts or even milliwatts to a modest antenna, operating can become **very tedious and frustrating if you do not know what to expec**t, given your antenna and the current state of the ionosphere. A bit of study can lead to the knowledge that makes a 600km range for most of your QSO's a pleasing success. It can lead to an understanding of why your call/QSO DX ratio is only 1 in 18, and that the "1" is actually a minor miracle! I should note that the "**for QRP DX'rs**" phrase in the title has to be read carefully -- when K0ZK with his Rockmite at 420mw in ME or AA4XX in NC with 250mw work you, they are QRP DX'rs and you are the DX! And both of you have an opportunity to learn something new about ionospheric propagation under the current conditions (SFI, Ap-Index) for that specific path. [QSO 4/11/2011 0725 10106.8Mhz **P29NI** 579 to **W0RSP**, 3rd call; SFI=105, Ap=02]

Ade Weiss W0RSP (ex-K8EEG)
11 April 2011

****

ISBN 0-9614139-0-6

Dedications

M. Walter Maxwell W2DU already is a legend in his own time because of his tireless and outstanding contribution to radio amateurs' understanding of r.f. wave behavior on transmission lines and his debunking of misconceptions of the nature and effect of SWR that have plagued the hobby since the invention of the so-called "SWR Meter". Beginning with his series of seven papers titled "Another Look at Reflections" published in *QST* (April 1973 to August 1976), Walt Maxwell clearly and precisely explained and demonstrated the theorem of conjugate matching in regard to the input and output terminals of a transmission line. In July 1990, the ARRL published the revised series of papers along with several additional chapters in **Reflections,** which went through two printings. Due to a controversy originating in *QST* about conjugate matching, the ARRL technical staff decided to not publish a second edition, and, in fact, deleted Maxwell's contributions that had been in the **ARRL Handbook** from 1986 through 1994. In the second edition **Reflections II** (published by **World Radio** in 2001), Maxwell added the new Chapter 19 refuting the contention that no conjugate match was possible in a system fed by an vacuum tube r.f. amplifier. His argument and demonstration was examined and approved by a group of professionals whose names I know only because of their prominence; but I have enjoyed several conversations with retired Collins Engineer Warren Amfahr, E.E., W0WL, to whom I am indebted for positive comments about one of my presentations about SWR. On a more personal level, in 1983 I had the audacity to send a copy of three chapters of **The QRP'rs Guide** to Maxwell for his comments on my material. It seemed a natural student-teacher action since everything I had written about transmission lines and SWR was learned from his papers. And some was not, so it could have been wrong. It was astonishing to receive back a long letter clarifying some of my errors. The manuscript was marked up in pencil with a large number of corrections of content and suggested revisions. However, 5 pages were missing – he noted that he needed more time to deal with the issue of revising them. A while later, another letter included the missing pages with Walt's honest and direct comment that my method was incorrect and it produced incorrect results, and that there was no way of revising other than to delete the section and start again. To aid in the process, he included the artwork for **Fig. 2-18** along with the explanation that was needed. He also included an accurate original pencilled graph of the line loss attenuation of various types of feedlines and a modified Smith Chart vector graph from the *QST* papers. In terms of my reaction, bear in mind that this guy who was taking the time and energy to teach me the correct concepts was RCA's chief engineer solely responsible for the design of antenna systems for more than 30 earth-orbiting satellites (mostly QRP?) and assisted in the design of many others – including the TV dish on the Apollo lunar rover. Since then, I have added material to that which Maxwell corrected and I hope that it reflects a more enlightened understanding of what Maxwell was trying explain to me.

Robert B. Rose K6GKU, then Head of the Naval Ionospheric Assessments Systems Branch, began sharing his experience with QRP operation and his professional knowledge of propagation in **The Milliwatt: National Journal of QRPp** in the early 1970's. Looking back on the evolution of the QRP movement, the most important paper ever published in **The Milliwatt** was K6GKU's "*Ideas on a Method to Determine Short*

Term Changes in H.F. Propagation" (August 1974 issue) which is reprinted here in Chapter 3 section **3.42**. It was not merely a significant contribution to the QRP'rs knowledge of propagation predictions, but in fact was one of those seminal statements that change the course of history in regard to a specific discipline or area of study. Until then, the R12 smoothed average sunspot number was the unquestioned basis of propagation prediction methods. That was changed by Bob's argument that the 10.7cm solar flux provided a more accurate and much more current indication of solar activity and the state of the ionosphere. Of course, many readers of the paper in **The Milliwatt** started using the SFI as their index immediately. As I note in section **3.43**, *QST* joined us five years later. By 1 May 1983, K6GKU could look back and say in a letter: "Today it is now an accepted substitute for sunspot number in military and most amateur circles. After all the 'heat' I took on that one when *we* first published the idea in **The Milliwatt**, I now enjoy knowing *we* were right all along. In fact, most of the crazy ideas we proposed then came to pass." I italicise the "*we*" because it actually was Bob who was responsible – I just published the paper. In fact, this book is the result of his paper – a lot of us QRP'rs "saw the light" for the first time and started digging for more information about propagation. Then came K6GKU's release of **MINIMUF 3.5** in *QST* (see Chapter 1 section **1.25)**. As I mentioned above in the "Preface", Bob read the whole typescript of **The QRP'rs Guide** but extensively edited the chapters about propagation to update and correct them. He even offered to provide updated data and raytraces for my examples. I have since expanded those chapters and updated them, so some errors may have crept in around the core that Bob edited. I am indebted to him for that tedious job as well as his note that the reader would be overwhelmed with all the data, but it is data that QRP'rs should be aware of in order to understand the factors involved in h.f. communication with low powers.

Ade Weiss W0RSP (ex-K8EEG)

Ionospheric Propagation, Transmission Lines, and Antennas for QRP DX'rs

CHAPTER 1. Path Losses, Ionosphere Propagation Overview and Refraction, Computer Propagation Analysis.

CHAPTER 2. Antennas, Transmission Lines, and SWR.

CHAPTER 3. Formation and Structure of the Ionosphere.

CHAPTER 4. The Propagation of H.F. Radio Signals in Real ionospheres.

BOOK REVIEWS

maximum amount of transmitted power that can be dissipated in the circuit before communication ceases, and thus the minimum amount of power that must be radiated (i.e., "*e.r.p.*" or "effective radiated power", i.e, "power that can perform work"). **Fig. 1-1** makes clear that the actual output from the transmitter is *not* the effective radiated power because three resistance components are between it and the ionosphere on each end, namely, an optional antenna tuner which can exhibit a small loss, the transmission line, and the antenna itself. These losses must be taken into consideration in determining the actual "effective radiated power. The ionospheric losses are represented by the "**Hop 1 Path**" box and "**Path**" box for "**Hops 2,3,4,n**" where the "Ground/Sea Reflection Loss = 0.1*dB* to 9*dB*" per hop. The "Paths" box shows the 5 combinations of D-layer, E-layer, and F-layer loss resistances that are labeled circuit **A, B, C, D**. For example, when the TX station is in complete darkness and both the D-layer and E-layer have dissipated, the signal travels directly to the F-layer as in circuts **A** and **B**, where the RX station is in daylight and both the D-layer and E-layer are present with corresponding losses.

Fig. 1-1. Path Losses and Various Ionospheric Loss Circuits.

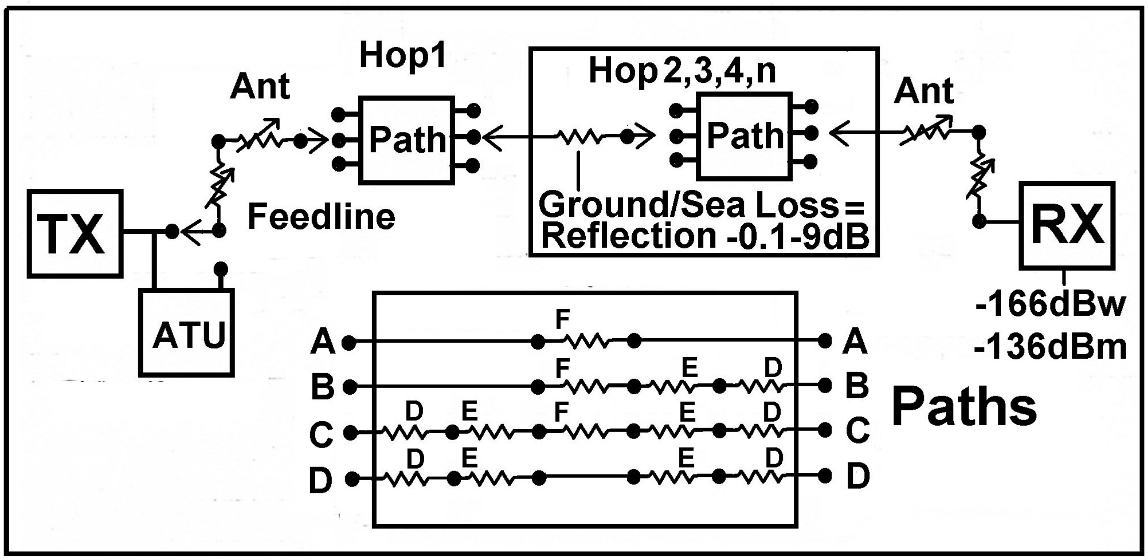

1.2) Receiver Sensitivity: *dBm*, *uv*. The one watt power level is a standard reference level against which path loss and resulting signal strength is measured. Path loss is stated in decibels, or "*dB*" and the resulting signal strength in "decibels relative to one watt", or "*dBw*". However, in low level circuitry like a receiver, 1 watt is awkwardly large (i.e., $2.33\text{x}10^{-17)}$ for describing signal levels. Thus, receiver sensitivity previously was universally given in microvolts, i.e., "*uv*" across 50ohms, but since the 1970's, the power available at the receiver terminals (and other aspects of receiver performance involving very low signal levels) is referenced against *one milliwatt* in "decibels relative to one milliwatt", or "*dBm*". Since one milliwatt is 1000 times less than one watt, and a power ratio of 1000 corresponds to a 30*dB* difference, *dBw* is easily converted to *dBm* by merely subtracting 30 from the *dBw* value, or (*dBm* = *dBw* – 30). Power density *Pd* in watts/meter^2 is calculated by:

height extends from about 110km to 220km. The virtual height rises sharply -- a function of retardation as the topside of the layer is reached. The F1-layer rises rather continuously from 220-450km. The F2-layer appears to be below the peak of the F1-layer, but this illusion is due to the cumulative group retardation that the wave experiences in passing thru the E- and F1-layers. At about 6.9 Mhz, the virtual height of the F2-layer rises sharply to its maximum, again a result of cumulative retardation. The actual height of wave penetration is much less than the virtual height and can be readily calculated. In this example, the actual time for equivalent free space travel for the E-layer maximum virtual height is equal to 110km actual height. However, as far as the horizontal distances are concerned (as in the ray-path of **Fig. 1-4)**, the wave appears to refract at the virtual height.

1.12) Baker Lake, High Latitude Winter Ionosphere. Next, an ionogram for a high north latitude in winter is shown in **Fig. 1-7**, taken at Baker Lake (64ºN geographical, 73ºN DIP latitude) with the running 12-month sunspot number at 160. The diurnal variations in ionization and virtual heights are represented by the three curves for 1200, 0000, and 0600 local solar time. The curve for 1800 is similar to 1200 but is not shown: the *foF2,* or *F2 critical frequency,* has dropped to 7.8Mhz and the virtual heights have risen 20km. Note the implications for winter paths to EU thru the high dip latitudes during high solar activity in the evening. With the E-layer gone after around 1600, low angle radiation has a clear shot to the F2, and as the F2 readjusts upward, the single hop distances increase dramatically. The reason for higher ionization at 0600 than at 0000 might not be apparent. As sunrise occurs to the east, ionization pushes westward along the magnetic dipole lines (*DIP latitude*) ahead of actual sunlight. Thus Baker Lake has already experienced a rise of about 2Mhz in *foF2* before the sun has risen.

Fig. 1-7. Ionosphere Model 3 Ionogram., Baker Lake. 73ºN. DIP

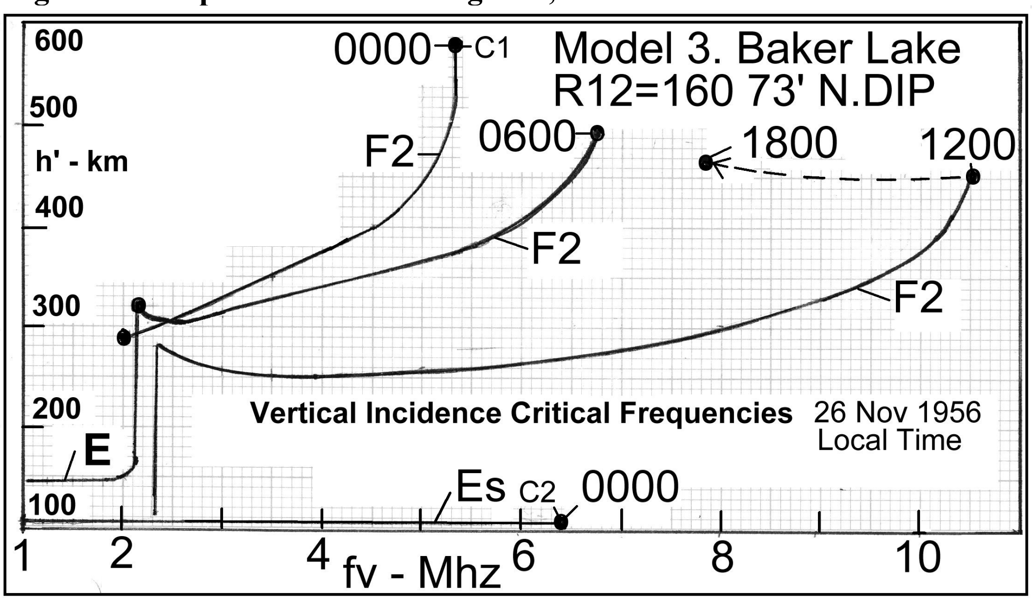

1.13) Grayline Zone at Sunrise and Sunset, and *Pedersen Propagation*. This effect can been seen in the *MUF(3000)F2* map shown later in **Fig. 1-12.** In the *grayline* zone at the left which represents the sunrise period, note that at north latitudes, such as about 43º N those signal levels should be reached. At the head of the list, the FMUF's for the IY2ARI QSO are 3Mhz below 21Mhz, but the **"B"** flag is present, so the FMUF might be higher less than 50% of the time. In regard to the SP8HFM QSO, approximately the same numbers appear, but note that at 2030Z, the "**B**" flag disappears, lowering the probability to the 0-10% of the time level. The OH4RH again shows an FMUF of 3Mhz below signal frequency at the time of the QSO, but the "B" flag is present. Finally, "A" flags appear for the EA8AGF and HA5KF paths -- the EA7CH QSO is shown and exhibits numbers

Fig. 1-17. 9 QSO's Prior to the W0RSP - S52R QSO.

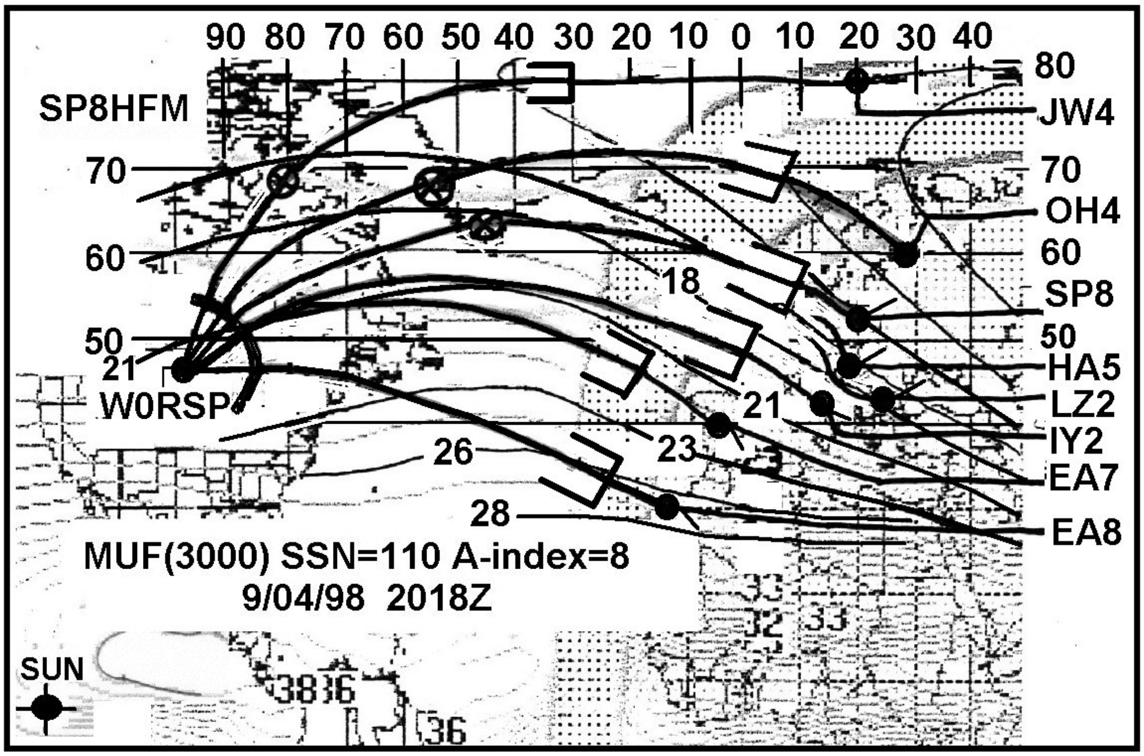

similar to the EA8AGF QSO. Finally, the LZ2BK and HA5KF predictions illustrate why the *QST* graphs and *CQ* tables were fairly worthless. The two locations are separated by only a few hundred km, only a fraction of the difference between midwest locations such as SD and Chicago. Yet the impact of that distance upon path geometry is profound. The LZ4KF predicted FMUF's are almost 2Mhz below those for the HA5KF path, and the probability flags are "**B**" instead of "**A**".

Overall, of these QSO's , only the predicted openings for EA8AGF and EA7CH seem very probable, that is, the actual FMUF's should be above the predicted level more than 50% of the time with the indicated signal levels. In regard to the *MUF(3000)* map contours, only the EA8AGF and EA7CH paths ought to have been open. In both cases, the probability should be close to or exceed 100%. But the other paths are predicted with fatal doom by both the map contours and the **MINIPROP** predictions. What is the "key" to meshing actual results with predictions? About 20 days later, the flux was around SFI = 150, so all of these paths showed a much higher FMUF and probability of being open. But nothing could be heard. A solar flare had pushed the A-Index up to 143 and higher! Black-out! Not even the most sophisticated propagation prediction program somehow developed the impression that when the high bands are either dead or activity-less, a DX station is likely to give a couple of trial "CQ's" not at the very bottom of the band, but around or above the 25Khz point – maybe a strategy to be calling every US

Fig. 1-24. Great Circle Path for W0RSP-VP5/AC8W

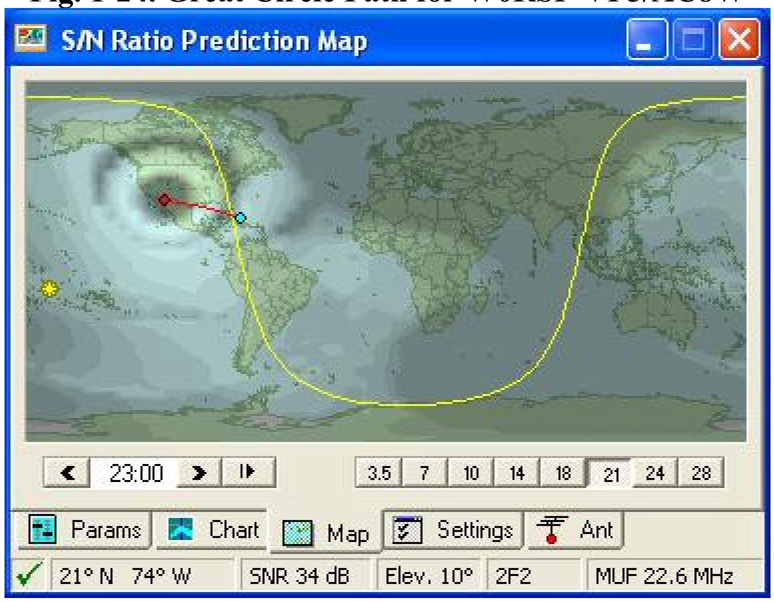

Fig. 1-24B. W0RSP - JW9VDA Path in "Pseudo" Color.

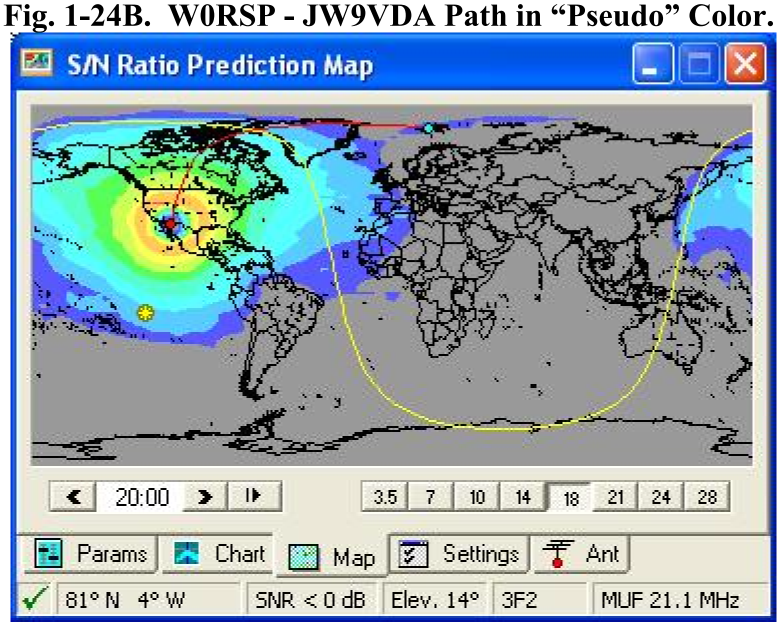

category including General Class licensees. At any rate, around 2250, I started hearing some stations down the band, and tuned down and found a pile-up of JA's, many of whom were 589 or so. I RIT'ed down until VP5/AC8W boomed in at 599+. So I loaded **HamCap** and entered VP5 and the 1-watt power level and the SSN was at 60. **Fig. 1-24** showed a phenomenal 34*dB* SNR, an unrealistically low radiation angle of 10º and an an aluminum foil shield outside the braid prevent such deterioration. The amount of loss from dielectric deterioration can be easily measured after a couple years of use.

It requires nothing more than (1) a QRP in-line Breune circuit r.f. wattmeter calibrated for accurate power measurements at 1 watt increments or less (see MFJ Enterprises's MFJ-813 $39.95, or build one – the **ARRL Antenna Book** usually has a Breune circuit unit project, or see my **Joy of QRP: Strategy for Success**, 1st or 2nd edition, pp. 144-149 for a QRP design); and (2) a commercial 50-ohm dummy load or a homebrew unit such as a pair of 1-watt or 2-watt 100-ohm carbon (regular brown type with color bands) resistors spliced in parallel and soldered with "zero-length" leads to the center conductor tube and the shell of a PL259 coax plug (or whatever type of plug mates with the transceiver output socket). Measure the resulting dummy value accurately; if it is too low, i.e., 49.3 ohms, a small triangular file can be used to file a shallow notch into each resistor and raise the resistance, the resistance measured again, and the process repeated until the load resistance is the same as the *Zo* resistance specified in the data list for the transmission line type. Unfortunately, if the dummy load measures *above* the *Zo* resistance, there is no way of decreasing the resistance. So, measure the resistor/s carefully to start with. Once the process is successful, connecting the coax to the dummy load then constitutes a "matched line" condition which exhibits no reactance. The testing process has two steps.

(1) First, the 50-ohm dummy load is connected with a 3-inch or so piece of good coax (length not critical) through the Bruene wattmeter to the transmitter and power output into the dummy load is adjusted to a given level and noted.

(2) Second, the wattmeter and dummy load are transferred to the far end of the coax cable being tested and without changing the transmitter output, the amount of power registered by the wattmeter is noted. If the coax is still in fine shape, the recorded power at both ends will vary very slightly for a 100-foot run of "matched coax" at the signal frequency, and even less for a 50-foot run. Use the "matched loss" figures for that type of coax as the standard – for example, consult the above referenced Carolina DX Association calculator or take the matched loss values from a **Table 2-2** type of data table. If the measured power, converted to a *dB* loss by the standard power ratio formula formula:

$$Loss(dB) = 10*log\ (P1/P2)$$

is greater than the matched loss specified in **Table 2-2** or similar lists, the dielectric deterioration is in progress and only speeds up. Results can be surprising. My old-standby 60-ft piece of RG8X foam dielectric that had been used for years because it "was a good cable" and "looked great" ended up soaking up 0.9 watts from a 3-watt 10.1Mhz signal! That figures out to a loss of 1.55*dB* or about 30% of the signal. If this were Tandy RG58 coax, that would amount to an additional 0.55*dB* loss (about a 50% increase) over that shown in **Fig. 2-1** at 10.1Mhz (see line "X") with a total loss at 28Mhz of about 2.6*dB*, approaching the 50% loss level! Then add 40 feet more loss to arrive at the 100-foot matched loss figure. The results can also be positively surprising. I still have a 28.4-foot hunk of Stancor 2014 RG8/U with a velocity factor = 0.66 laying around. It can be modeled in **EZNEC** and the calculated *R +/- jX* values then entered as in the **Fig. 2-3** screen where "*Ant. R*" = *98.5*, and "*Ant. X*" = *-j95*. The length of transmission line to the transmitter end is referenced in degrees of a wavelength (left column) and the corresponding lengths in feet and meters, and calculations are performed at intervals of 5-degrees.

TABLE 2-3. 40 Meter Dipole at 30-foot Height on 21Mhz.

Deg.	Feet	Metres	E(in)	Phase	I(in)	Phase	R(in)	jX(in)	Z Phase	Z
0°	0	0	43.6	316	0.32	0	98.5	-95	-43.96	136.85
5°	0.59	0.18	38.13	325	0.33	2	93.9	-69.52	-36.52	116.84
10°	1.18	0.36	33.61	337	0.33	3	90.83	-44.86	-26.28	101.3
15°	1.78	0.54	30.65	352	0.33	5	89.12	-20.7	-13.08	91.49
20°	2.37	0.72	**29.8**	**8**	**0.34**	6	88.67	3.22	2.08	88.72
25°	2.96	0.9	31.26	25	0.33	8	89.45	27.18	16.9	93.49
30°	3.55	1.08	34.71	38	0.33	9	91.52	51.45	29.34	104.99
35°	4.14	1.26	39.53	49	0.32	11	94.98	76.31	38.78	121.84
40°	4.74	1.44	45.18	58	0.32	12	100.04	102.05	45.57	142.9
45°	5.33	1.62	51.24	64	0.31	14	106.98	129.02	50.33	167.6
50°	5.92	1.8	57.43	69	0.29	16	116.27	157.57	53.57	195.82
55°	6.51	1.98	63.54	74	0.28	18	128.56	188.1	55.65	227.83
60°	7.1	2.17	69.44	77	0.26	20	144.79	221.04	56.77	264.24
65°	7.7	2.35	75.02	80	0.25	23	166.36	256.82	57.07	305.99
70°	8.29	2.53	80.191	82	0.23	26	195.33	295.74	56.56	354.42
75°	8.88	2.71	84.89	85	0.21	29	234.82	337.73	55.19	411.35
80°	9.47	2.89	89.05	86	0.19	34	289.48	381.76	52.83	479.1
85°	10.06	3.07	92.63	88	0.17	39	366.06	424.34	49.22	560.41
90°	10.66	3.25	95.59	90	0.15	46	473.37	456.55	43.96	657.67
95°	11.25	3.43	97.9	92	0.13	55	619.08	458.37	36.52	770.3
100°	11.84	3.61	99.54	93	0.11	67	796.58	393.38	26.28	888.42
105°	12.43	3.79	100.49	95	0.1	82	958.21	222.56	13.08	983.72
110°	13.02	3.97	**100.75**	**96**	**0.1**	98	1013.7	-36.86	-2.08	1014.38
115°	13.62	4.15	100.31	98	0.1	115	921.06	-279.89	-16.9	962.65
120°	14.21	4.33	99.17	99	0.12	128	747.24	-420.07	-29.34	857.22
125°	14.8	4.51	97.34	101	0.13	139	575.87	-462.64	-38.78	738.69
130°	15.39	4.69	94.85	102	0.15	148	440.86	-449.75	-45.57	629.79
135°	15.98	4.87	91.72	104	0.17	154	342.76	-413.36	-50.33	536.98
140°	16.57	5.05	87.98	106	0.19	159	272.9	-369.81	-53.57	459.6
145°	17.17	5.23	83.67	108	0.21	164	222.9	-326.13	-55.65	395.03
150°	17.76	5.41	78.84	110	0.23	167	186.63	-284.92	-56.77	340.6
155°	18.35	5.59	73.55	113	0.25	170	159.91	-246.86	-57.07	294.13
160°	18.94	5.77	67.88	116	0.27	172	139.95	-211.89	-56.56	253.93
165°	19.53	5.95	61.91	119	0.28	175	124.9	-179.64	-55.19	218.79
170°	20.13	6.13	55.76	124	0.3	176	113.5	-149.68	-52.83	187.85
175°	20.72	6.32	49.58	129	0.31	178	104.9	-121.6	-49.22	160.6
180°	21.31	6.5	43.6	136	0.32	180	98.5	-95	-43.96	136.85

Alternately, actual measurements of the antenna terminal impedance made with an RX-Bridge or an MFJ "SWR Analyzer" (MFJ-249B, $269.95) or the handheld Autek Research "VA1 RX Vector Analyst" (www.autekresearch.com, $199.95) which displays up to a dozen functions including the "*R +/-jX*" complex impedance, which can be entered into the "Transmission Line Performance" program at the "*Ant.R*" and "*Ant.X*" prompts In one of my previous locations, some of my antennas were chimney-supported and the input terminals actually measured directly at the actual height above insertion or removal of an extension takes advantage of the line's impedance transformation ability, most notably in regard to the steep-slope swings in resistance and reactance that usually happen along very short portions of a transmission line (see **Fig. 2-4**). This is especially useful because most QRP'rs who use parallel line do so in order to

Fig. 2-4. **Table 2-3 "R" and "+/-jX" Curves with "Zero Reactance" Points A, B**

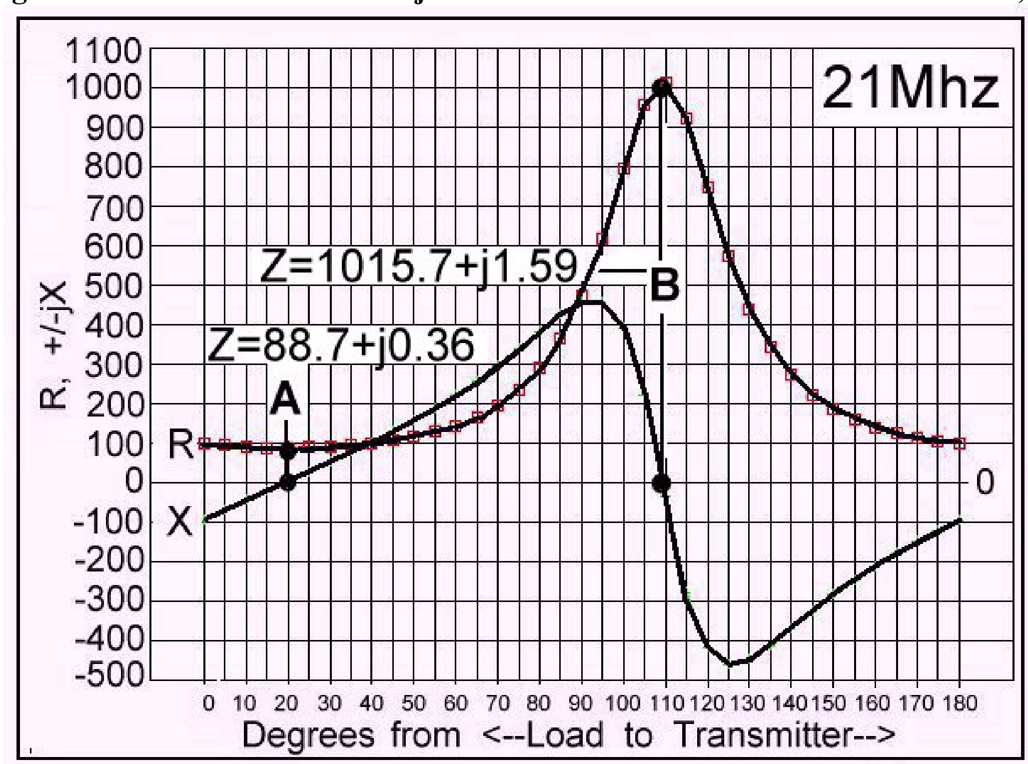

be able to tune a single antenna on multiple bands. But switching from 40 meters to 30 meters on a 40-meter dipole can create interesting line input impedances that are out of the balanced tuner's range. The example antenna used in the present discussion (40 meter dipole up 30 feet above poor ground, fed with 51 feet of 300-ohm ladder line) does present difficulty to the Emtech ZM-2 on the 14Mhz band. I have the set of two extension lines "in case" which solve the problem and move the feedline input terminals away from the wildly-swinging impedance zone of the line. However, my homebrew balanced tuner (see below), switchable between parallel and series tuning, with two selectable separate coupling links, handles the bands 40-10 meters without difficulty and will tune the 40 meter dipole to 80 meters but with fairly critical settings. Since 15 meters is the third harmonic of this dipole, its settings are very similar to those of 40 meters, but 30 and 20 meters require significant readjustment, as would be expected.

2.26) Parallel Lines and Baluns. Suppose that an antenna with a parallel transmission line length of 180º + 120º (see **Table 2-3** for 120º value, which reappears every additional 180º along the line) is being used to minimize line loss and the complex impedance at the transmitter end is *ZL = 747 –j420* ohms. The typical internal transmatch most probably will not match 50 ohms to that impedance, and furthermore, is not designed to handle balanced feedline connections. So, various schemes of employing a about 0.039 wavelength and about 0.4 and 0.53 wavelength heights. Generally, the illustrations in the handbooks omit the variation in reactance, graphing just the radiation resistance.

Fig. 2-16. Radiation Resistance, Reactance Over "Perfect Ground" vs. "Real Ground.

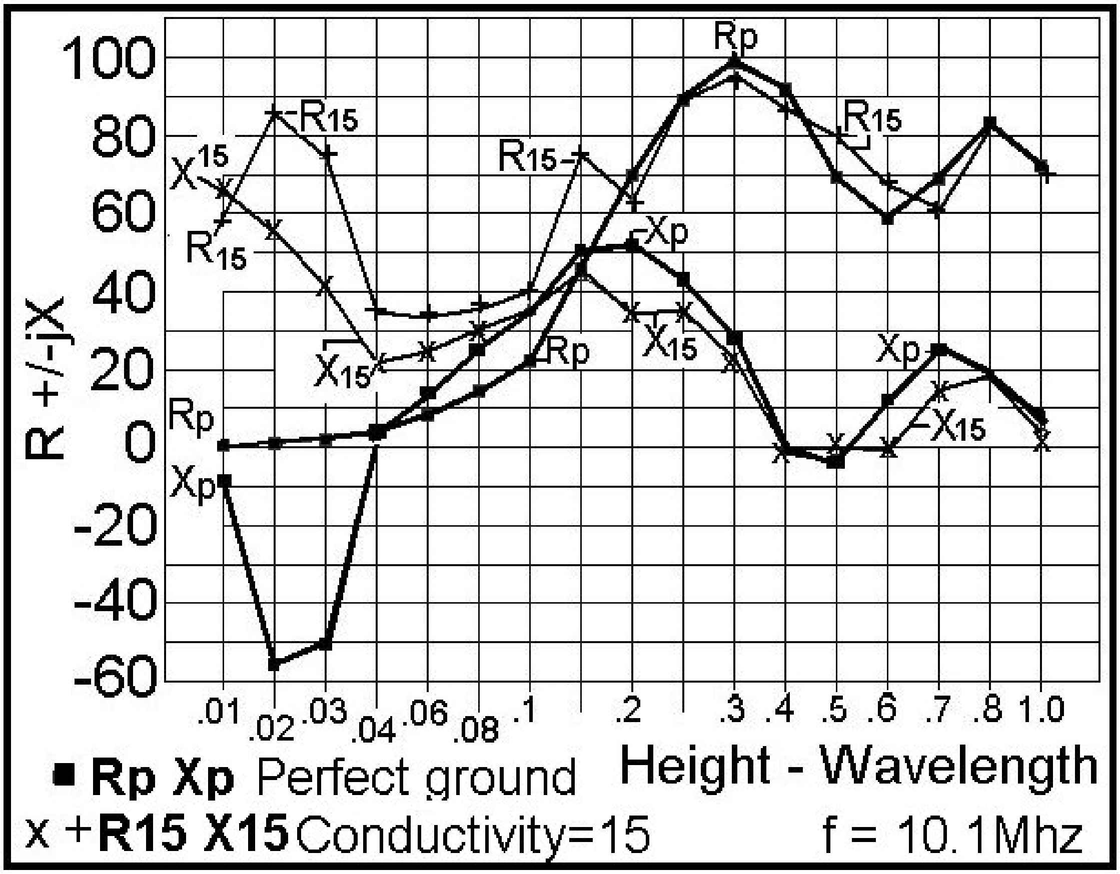

2.58) Over Real Ground. The **R15** and **X15** curves over "real ground" with a conductivity = 15 are more interesting because they represent almost all real antennas interacting with ground. At 0. 2 wavelength height, **R15** diverges from **Rp** as it rises to 75.3 ohms, dropping to 40 to 35 ohms between 0.1 and 0.04 wavelengths height, rising to 85.5 ohms at 0.02 wavelengths and finishing at 58.3 ohms. The most significant fact is that *the difference* between the "perfect ground" and "real dirt" radiation resistance curves below the 0.2 wavelength height *is comprised of the absorption of the wavefront* in the lossy dirt medium under the antenna. So, at the 0.15λ height, the "real ground" radiation resistance is 75.3 ohms in contrast to the "perfect ground" value of 45.7 ohms. The difference is 29.6 ohms or about 40% of the total of 75.3 ohms. On 10.1Mhz, the 0.15λ height = 14.6 feet, which is lower than the usual "low antenna" height for 30 meters. For lower frequency antennas, the 0.15λ height in feet increases as expected, i.e., 21.7 feet on 7Mhz, 41.9 feet on 3.5Mhz, and 82.3 feet on 1.8Mhz.

The difference in the reactance curves in the same region is not significant – both the *Xp* and *X15* curves exhibit roughly equal magnitudes although differences in sign. But this reactance adds to the mismatch loss caused by the height-related ground loss. Thus, every degree of movement back from the reflection point. This is the angle of the coefficient of reflection **ρ** for the point $d = 45^o$ back from the load. The summation of the vectors yields the resultant *line* voltage $E = 1.414$ at 0^o.

Fig. 2-18. Open-Circuit Vectorial Summation at 0º → 90º Points Back on Line. (Provided by Walter Maxwell W2DU)

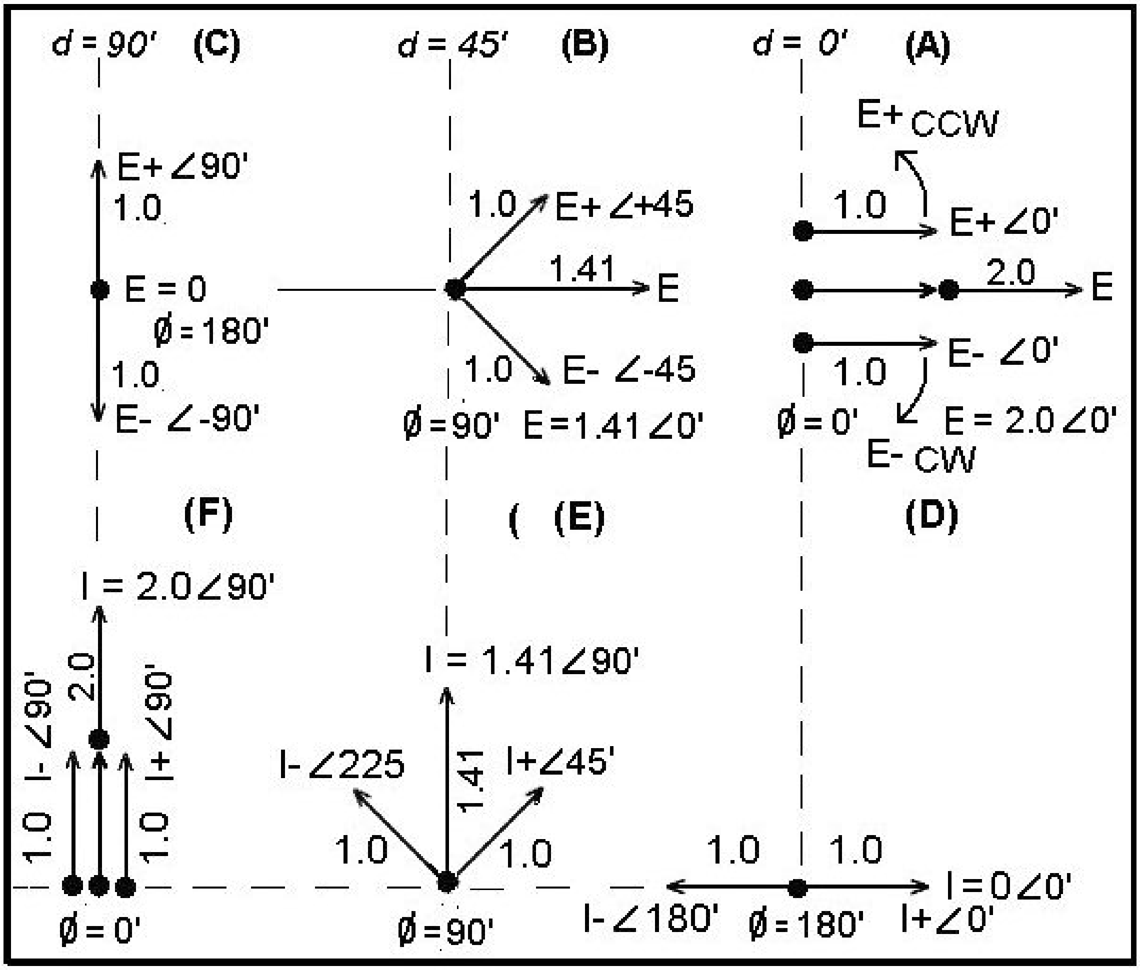

The combined two vectors are shown at the $d = 45^o$ point back from the reflection plane in **Fig. 18B**. The 45º counter-clockwise rotation of the *E+* vector and the 45º clockwise rotation of the *E-* vector produce the 90º "enclosed" angle as shown in **Fig. 18B**. (This is the angle of the coefficient of reflection **ρ,** which for the point $d = 45^o$ is twice the distance back from the load or 90º.) The angle of the resultant *line* voltage component $E = 1.414$ remains at 0º phase angle, as it will up to the $d = 90^o$ point. As the vectors continue their rotation, the "enclosed" phase angle increases and the resultant vector shrinks until the $d = 90^o$ point. At that point, each vector has rotated 90º so that the resulting "enclosed" angle is 180º (= angle of the coefficient of reflection **ρ**) forming a straight line with the vectors pointing in opposite directions as shown in **Fig. 18C**. At the coefficient reflection angle of 180º, the exactly-opposite phase vectors cancel and the resultant drops to $E = 0$ at $d = 90^o$. For an open termination, then, the *line E maximum* occurs at the load, and the *line E minimum* at the $d = 90^o$ point back from the load. The pattern of line voltage and current distribution along a transmission line terminated in a resistance. Bear in mind that there *is* a "standing wave" because of the phase relationships and the resultant current and voltage components vectorially summing along the line to produce a value for each point on the line. The pattern is the same, regardless of whether curve **A** reactance changes every $d = 90^o$ whether the "count" begins at $d =$

Fig. 2-22. R, jX, Ephase, Iphase Curves for Purely Resistive Load *ZL= 16.7 +/-j0.*

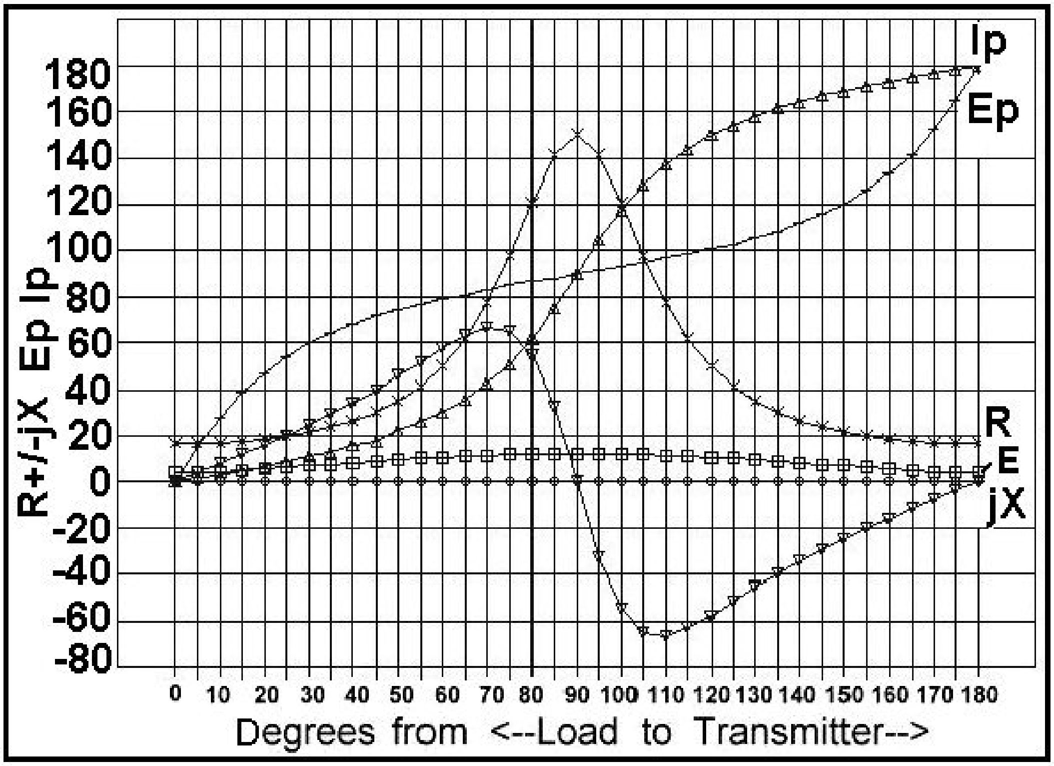

0^o or somewhere else on the line. As a result, in non-resonant antennas, i.e., those with reactance as well as resistance in the terminal impedance, there are *two* zero-crossing points where the shift goes from $+jX$ to $-jX$ and back to $+jX$ on a $d = 180^o$ transmission line. The graphs for the 7Mhz dipole discussed earlier illustrate this point. However, the location of the maximum and minimum points of the pattern do shift because of changes in reactance. The appearance of reactance at the antenna terminals inevitably causes such

Table 2-7. Mismatch Case Where *ZL < Zo*. *ZL = 16.7 –j0.*

		Zo=50 ZL=16.7 -j0			1w	1Mhz		
Degrees	**E(in)**	**Phase**	**I(in)**	**Phase**	**R(in)**	**X(in)**	**ZPhase**	**Z**
0º	**4.09**	**0**	**0.24**	**0**	**16.7**	**0**	**0**	**16.7**
5°	4.21	15	0.24	2	16.81	3.88	13.00	17.26
10°	4.55	28	0.24	3	17.16	7.81	24.46	18.85
15°	5.06	39	0.24	5	17.76	11.81	33.62	21.32
20°	5.68	47	0.23	7	18.64	15.93	40.53	24.52
25°	6.36	54	0.22	9	19.85	20.22	45.53	28.34
30°	7.07	60	0.22	11	21.47	24.73	49.04	32.75

voltage E leading the current I. The initial $d = 0^o$ *Ephase* angle value is repeated at the $d = 180^o$ point and reversed at the $d = 90^o$ point.

(5) The addition of a capacitive reactance component $-jX$ in the $ZL < Zo$ case reverses the $+jX$ shifts, i.e., "pushes" the ***R*** peak, *Emax, Imin,* and first and second zero-reactance crossing points back from the antenna terminals by an amount proportional to the amount of the added reactance $-jX$.

As a result, the line exhibits a capacitive reactance from the $d = 0^o$ point where the current I component leads the voltage E to the first zero-reactance crossing point, shifts to inductive, and then back to capacitive at the second crossing point. The initial $d = 0^o$ *Iphase* angle value is repeated at the $d = 180^o$ point and reversed at the $d = 90^o$ point. I should also note the obvious: a halfwave dipole is *not intrinsically a 50-ohm antenna*.

In short, the behavior of the traveling wave on a transmission line depends upon two sets of variables. The first variable is the type of the mismatch between the characteristic impedance of the transmission line and the resistance ***R*** exhibited by the load, that is, whether the former is greater or lesser than the latter. This establishes the basic resistive phase shift from the perfectly matched case where $ZL=Zo$. The second variable is the type of reactance exhibited by the load, i.e., whether capacitive or inductive. This determines how the resistive phase shift is modified by the reactance. Thus it is only partially true to state as found in two reputable sources:

"With a load having <u>inductive reactance</u>, the point of maximum voltage and minimum current is <u>shifted</u> <u>toward the load</u>. The opposite is true when the load reactance is capacitive."(p.24-9) or "<u>inductive reactance</u> <u>pushes</u> peak resistance down the line <u>away from the antenna</u>".

Actually, *both* statements are true although they seem to be directly contradictory -- each is true for one case of resistive mismatch, i.e, either ***ZL >Zo*** or ***ZL < Zo.***

Part 5. Transceiver, Transmatch, Transmission Line Terminal Impedance

2.93) Transceiver → Transmission Line Junction. The wave reflected from the antenna eventually arrives at the input end of the feedline which is connected either directly to the output network of the transceiver or to a transmatch inserted between the two. The reflected wave power is always less than the power being fed into the transmission line input terminals (unless an open-circuit or short-circuit has developed at the transmission line to antenna junction, in which case, the antenna is no longer connected). Net current flow therefore must be in the direction of the traveling wave exhibiting a greater magnitude. In other words, the reflected wave on the transmission line is re-reflected at the input terminals of the line, and becomes an incident wave, or more correctly, part of the new incident wave being fed into the transmission line.

Either the voltage component *E-* or current component *I-* experiences a 180° phase reversal upon re-reflection, depending on the case of $ZL>Zo$ or $ZL<Zo$, thereby reversing the phase shift caused by reflection at the antenna terminals. If $ZL = Zo$, the

entering regions of higher recombination rates, quickly undergo recombinations and are removed from the overall ion concentration picture. In other words, the relationship between the two layers is in a constant state of flux throughout hours of sunlight. Upper atmosphere heating also enters into the picture. An attempt at pictorially illustrating this process is given in **Fig. 3-14**. Once darkness sets in, with cooling of the upper atmosphere as well as collapse of the E-region ionization which supports the F1-layer, the F2-layer drops downward to assume its night time stance.

Fig. 3-14. Diurnal variation in F-Region N*max* and F2-*hmax*.

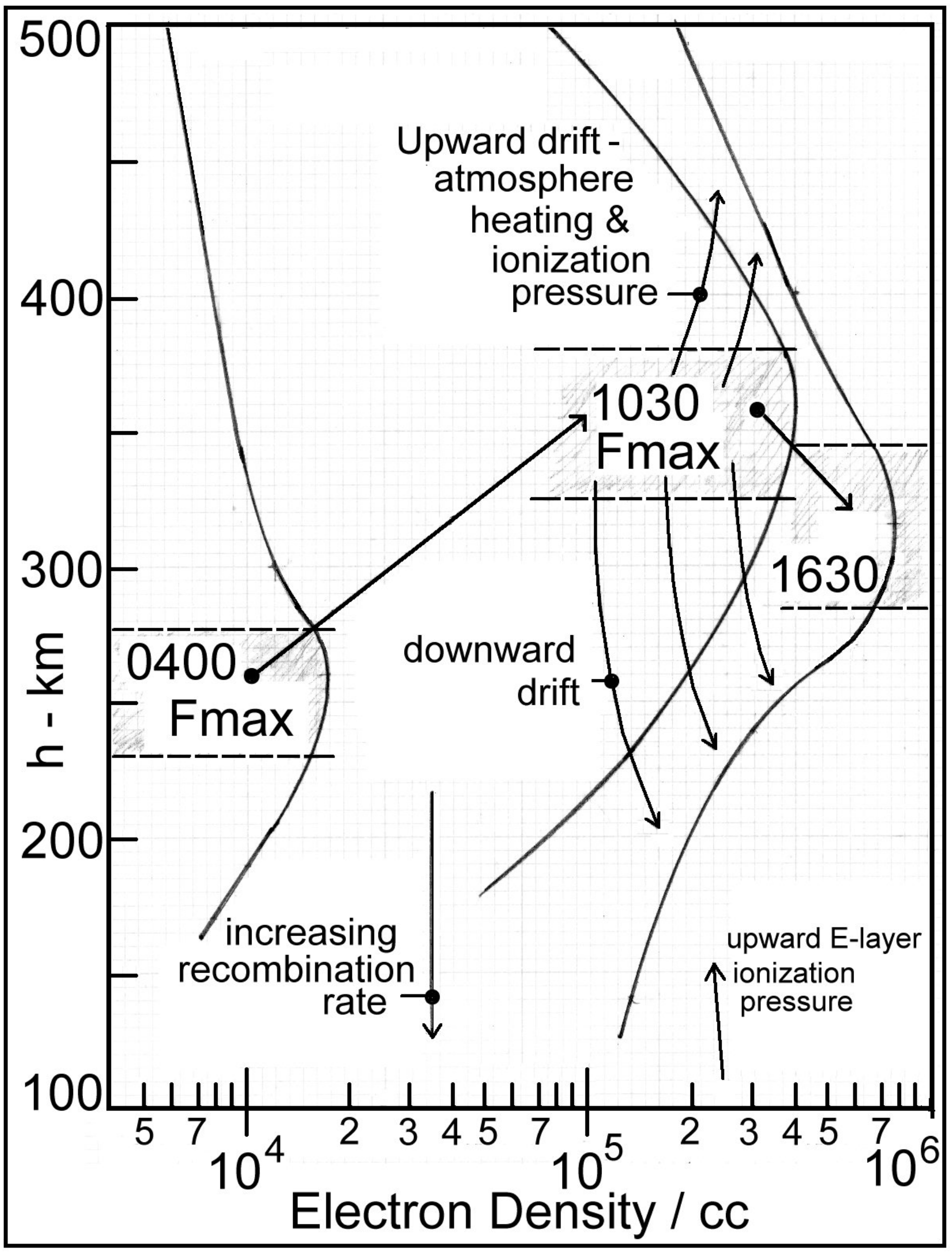

Fig. 3-14 is an artist's visualization of a dynamically changing ionosphere at three times during a 24 hour period. At 0400 local time, the ionosphere has reached its lowest

10.7cm flux showed a variation of about 111 to 189 units; for April, R12 stood at 70.7 while the flux varied between 130 to 196. During either month, then, actual ionospheric conditions on certain days would be comparable to sunspot numbers more on the order of about 60 and 150! The rationale for preferring the daily 10.7cm flux level SFI as an index is obvious.

Fig. 3-23 Correlation of Daily Solar Flux Index (SFI) and monthly SSN R12).

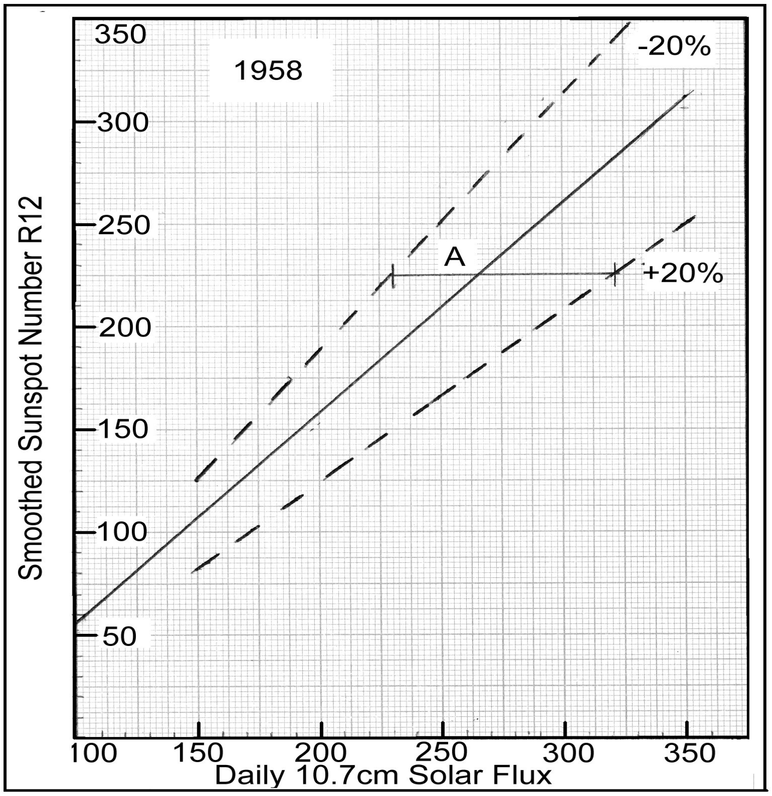

3.46) Solar Flux Mean Value vs. the 11 Year Sunspot Cycle. When the mean values of yearly solar flux measurements are correlated to the yearly running smoothed sunspot numbers (Rl2), the flux emerges as a short-term oscillation super-imposed upon the 11 year sunspot cycle pattern. This is implied by **Fig. 3-22**, where a rising sunspot number is accompanied by a rising flux level. The pattern traced across the 11 year sunspot cycle by the yearly mean values of solar flux follows the general pattern traced by the yearly smoothed sunspot number. Again, the variation between the daily flux level and an average of a longer period should be noted. The daily flux levels during a given year vary as much as 30% above and below the mean yearly value.

3.47) 10.7cm Solar Flux Intensity and Ionization Radiation Spectrum Intensity. As noted earlier, the 10.7cm radio noise emissions are produced by the same solar energy mechanisms as are responsible for the UV, EUV, and X-ray emissions that form the ionosphere. In addition, these photon emissions are responsible for other mechanisms in the formation of the ionosphere, such as heating which can produce shifts in vertical gas distributions and thereby affect propagation. The exact quantitative relationship between accordance with R12 numbers. The behavior of the equatorial F-region assumes seasonal and diurnal characteristics, then, in the general context of sunspot cycle relations.

3.104) Seasonal and Diurnal Variations in the Equatorial F-Region. F-region behavior at all latitudes is affected by the level of geomagnetic-disturbance obtaining at any given time. For purposes of establishing F-region patterns which reflect only the operation of mechanisms excluding geomagnetic disturbances, researchers rely upon data gathered during the "five quiet-days" per month selected by observatories because of the low geomagnetic activity level during those days. (The "**Ap** Index" ranging from 0 to 400 is the primary measurement of daily geomagnetic activity: experience shows that an **Ap**<11 equates with very good conditions for QRP DX'ing.) Then monthly mean levels of electron density and critical frequency are based upon quiet days data and used as the basis of studying F-region behavior. **Fig. 3-45** to **Fig. 3-48** use the measured 5 quiet days of monthly mean diurnal electron density variations for months of June, September, and November, 1957 (R12>180) to illustrate equatorial F-region behavior, but as noted earlier, a direct correlation between electron density and critical frequency exists, so that the curves represent critical frequency patterns in a crude manner. **Fig. 3-45** and **Fig. 3-46** present diurnal and seasonal variations in F-region behavior for two locations. Huancayo is located at 2°N. DIP (12.1°S geographic), right at the DIP equator, and the other at 13°N DIP, a position which places Talara at the northern rim of the equatorial trough which extends roughly 15° either side of the DIP equator. The curves represent a high solar-cycle epoch, with the R12 above 180 during the 1953-58 period shown. A

Fig. 3-45. Mean Diurnal Variation in *foF2* at Equatorial Location – Talara.

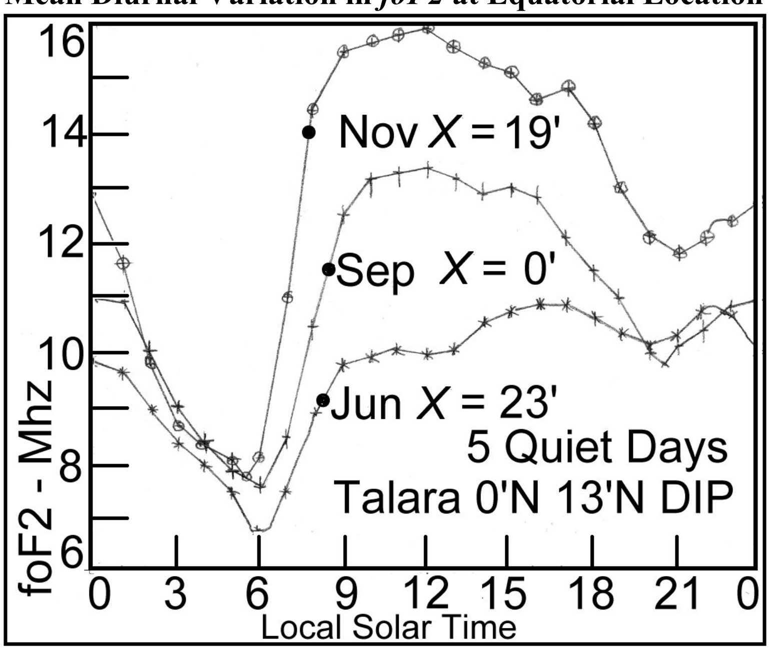

(After Somayajulu, 1964)

minimum sunspot epoch would produce similar curves, but with far less variation both seasonally and diurnally. Maximum *foF2* occurs in late equinox season (November) as the ionization build-up of equinox (September) peaks at this location on the geographic equator. As the sun moves south during winter, the Talara *foF2* remains higher than the antenna than in the flat-earth model's entry point **J**, which is at the same virtual height as indicated by the dotted line **JX**. Further, note that the entry point incident-angles are quite different. Compare the *Qin* formed by dropping a vertical reference (dotted line) from point **J** to **X** (flat-earth model) with the *Qin* at point **A** (curved-earth). In the curved-earth model, the vertical reference at a given point is established by a line such as

Fig. 4-22. "Curved-Earth" Model of the Ionosphere and Parameters.

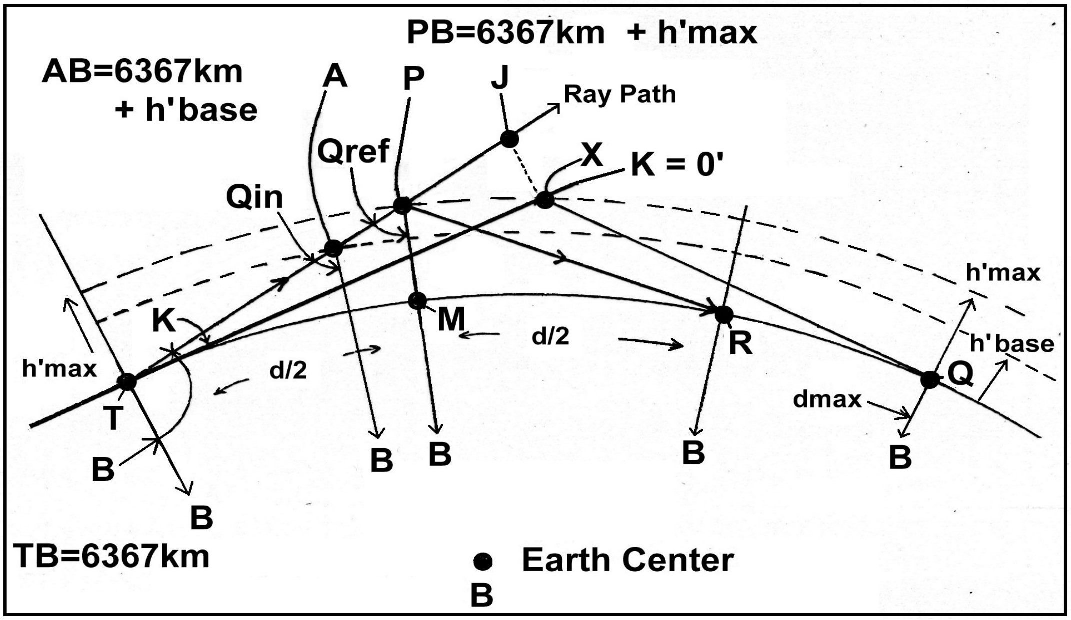

AB drawn from that point through the earth's center, and the resulting angle decreases with increasing distance of travel from the antenna. Thus, the incident-angle at point **P** is smaller than at point A because of the rotation of the earth-radius from distance **TA** to TP. In addition, as noted earlier (see section **4.20**, **Table 4-1**), in the curved-earth model, radiation angle K and incident angle *Qin* are no longer complimentary, and *Qin* and *Qref* are no longer equal, as in the flat-earth model. In turn, the shift in flat-earth to curved-earth geography and the resulting geometry shifts the relationship between geographical and electrical components through the incident-angle *Qin*. Since the curved-earth *Qin* is smaller than for the flat-earth model, the wave path must penetrate higher into the ionosphere before the ***n*** = *sinQin* refraction condition is satisfied.

4.46) Wave Path Calculations. Wave Path Calculations with the curved-earth model are more complicated because the simple right triangle geometry of the flat-earth model no longer obtains. Instead, oblique-triangle solutions using the Law of Sines and Law of Cosines, as well as solutions for arc-length on a circle, must be employed. The various quantities appear in **Fig.4-22** as follows.

(1) **Triangle Solutions.** As with the flat-earth model, it is with triangles representing half the total path, assuming a symmetrical path **TPR**. Triangle **TAB** represents path geometry to the point of entry at the base of the ionosphere, and is formed by earth-radius **R**, wave path **TA**, and line **PB**, which is the sum of the earth-radius and height of the E-Layer base *hE*. Incident-angle *Qin* is formed at point **A** by wave path **TA** and **AB**

4.60) Model 1, 21Mhz Reflectrix. The reflectrix curve shown in **Fig. 4-28** for a 21Mhz wave frequency is similar to the 14Mhz curve, but note that an *fv* capable of refracting a 21Mhz signal at K = 1.1° is not reached until a virtual height of 150km (**Fig. 4-24**), where *fv* = 3.7Mhz results in a *Qcrit(fv)* = 79.85°. This corresponds to a radiation angle of 1.1° in curved-earth geometry, and with *h'E* at 100km, the virtual path extends to the virtual refraction point at 1252km (2504km = total distance). The E-layer knee forms at 2381km, with K = 2.64°, and at 4.36°, the "break through" point at 2520km is reached.

Fig. 4-28. Model 1, 21 Mhz Reflectrix Curve.

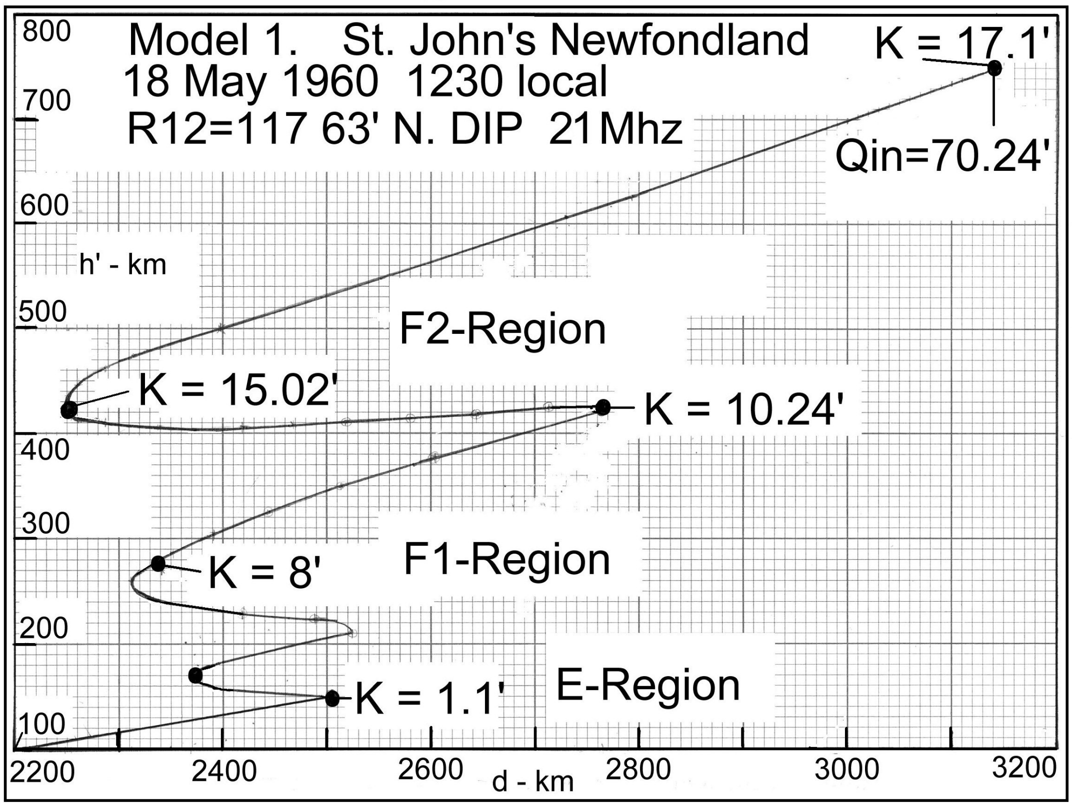

Note that these radiation angles are low in comparison to the 14Mhz curve, and in a practical context, rarely attainable in amateur practice due to "suck-in" in the "near zone" extending several hundred wavelengths beyond the antenna (Brewster angle = 14°). The F1-knee tip reverses at 2311km at K = 7.2°, and F1 distance extends to 2762km at K= 10.24° for transition from Fl- to F2-refractions. Even though F1-refractions require very low radiation angles, the 7° to 10° range is somewhat difficult but attainable in practice, bearing in mind that a 15-meter antenna up a full wavelength is at a height of only about 45 feet. Finally, the F2-curve duplicates that seen for the 14Mhz curve of **Fig. 4-27**. However, note that the maximum 21Mhz distance exceeds that possible with a 14Mhz signal via F2-refractions. This is because the highest radiation angle that will refract from this ionosphere for a 21Mhz signal is smaller than for 14Mhz, and hence, requires a longer journey at the lower radiation angle to reach the virtual refraction point at 750km.